

Statistical Analysis of the Impact of Anode Recess on the Electrical Characteristics of AlGaIn/GaN Schottky Diodes With Gated Edge Termination

Jie Hu, *Student Member, IEEE*, Steve Stoffels, Silvia Lenci, Brice De Jaeger, Nicolò Ronchi, Andrea Natale Tallarico, Dirk Wellekens, Shuzhen You, Benoit Bakeroot, Guido Groeseneken, *Fellow, IEEE*, and Stefaan Decoutere

Abstract—In this paper, we have extensively investigated the impact of anode recess on the reverse leakage current, forward voltage (V_F), and dynamic characteristics of Au-free AlGaIn/GaN Schottky barrier diodes with a gated edge termination (GET-SBDs) on 200-mm silicon substrates. By increasing the number of atomic layer etching (ALE) cycles for anode recessing, we have found that: 1) the reverse leakage current is strongly suppressed due to a better electrostatic control for pinching off the channel in the GET region; a median leakage current of ~ 1 nA/mm and an I_{ON}/I_{OFF} ratio higher than 10^8 have been achieved in GET-SBDs with six ALE cycles; 2) the forward voltage (~ 1.3 V) is almost independent of the ALE cycles, taking into account its statistical distribution across the wafers; 3) when the remaining AlGaIn barrier starts to be very thin (in the case of six ALE cycles), a spread of the ON-resistance, mainly attributed to the GET region, can occur due to the difficult control of the remaining AlGaIn thickness and surface quality; and 4) the dynamic forward voltage of GET-SBDs shows a mild dependence on the ALE process in pulsed I - V characterization, and a more ALE-dependent dynamic ON-resistance is observed.

Index Terms—200-mm, AlGaIn/GaN, atomic layer etching (ALE), diode, GET-SBD, leakage, metal-insulator-semiconductor high-electron mobility transistor (MISHEMT).

Manuscript received April 30, 2016; revised June 14, 2016; accepted June 30, 2016. Date of publication July 20, 2016; date of current version August 19, 2016. This project has received funding from the Electronic Component Systems for European Leadership Joint Undertaking under grant agreement No 662133. This Joint Undertaking receives support from the European Union's Horizon 2020 research and innovation programme and Austria, Belgium, Germany, Italy, Slovakia, Spain, United Kingdom, Netherlands. The review of this paper was arranged by Editor J. Mateos.

J. Hu and G. Groeseneken are with the Interuniversity Microelectronics Center, Leuven 3001, Belgium, and also with the Department of Electrical Engineering–Microelectronics and Sensors, Katholieke Universiteit Leuven, Leuven 3001, Belgium (e-mail: jie.hu@imec.be; guido.groeseneken@imec.be).

S. Stoffels, S. Lenci, B. De Jaeger, N. Ronchi, D. Wellekens, S. You, and S. Decoutere are with the Interuniversity Microelectronics Center, Leuven 3001, Belgium (e-mail: steve.stoffels@imec.be; silvia.lenci@imec.be; brice.dejaeger@imec.be; nicolo.ronchi@imec.be; dirk.wellekens@imec.be; shuzhen.you@imec.be; stefaan.decoutere@imec.be).

A. N. Tallarico is with the Advanced Research Center on Electronic System, Department of Electrical, Electronic, and Information Engineering, University of Bologna, Cesena 47521, Italy (e-mail: a.tallarico@unibo.it).

B. Bakeroot is with the Interuniversity Microelectronics Center, Leuven 3001, Belgium, and also with the Centre for Microsystems Technology, Department of Electronics and Information Systems, Ghent University, Ghent 9052, Belgium (e-mail: benoit.bakeroot@imec.be).

Color versions of one or more of the figures in this paper are available online at <http://ieeexplore.ieee.org>.

Digital Object Identifier 10.1109/TED.2016.2587103

I. INTRODUCTION

SCHOTTKY barrier diodes (SBDs) and high-electron mobility transistors (HEMTs) based on an AlGaIn/GaN heterojunction have emerged as promising candidates to replace silicon devices for high-power and high-frequency switching applications due to the superior material properties of GaN [1]–[6]. The combined wide bandgap of GaN-based devices and the 2-D electron gas (2-DEG) with high mobility and sheet density at the AlGaIn/GaN interface give rise to more efficient power devices compared with conventional silicon devices. Recently, the demonstration of high-performance Au-free AlGaIn/GaN SBDs and HEMTs on 200-mm silicon substrate has become a major breakthrough in the field of power electronics enabling the reduction of manufacturing cost [7], [8].

In the past few years, many research groups have been working on AlGaIn/GaN SBDs aiming at leakage reduction, forward voltage improvement, breakdown voltage (BV) enhancement, and so on. In the OFF-state operation of the GaN diode, an electric field peak is present at the corner of the Schottky contact (SC) leading to a high leakage current [9], [10]. Matioli *et al.* [11] proposed a 3-D lateral AlGaIn/GaN SBD by integrating a trigate MOS structure with the Schottky junction. A superior electrostatic control of the GaN channel was realized in this 3-D anode structure resulting in an ultralow leakage current of 260 pA/mm [11]. However, a high forward voltage and an early device breakdown (BD) were observed in this device. In [2], we demonstrated a topology of the AlGaIn/GaN SBD with gated edge termination (GET-SBD) by embedding a thin Si_3N_4 layer as the edge termination inside the anode trench. The GET-SBD architecture [schematic is shown in Fig. 1(a)] showed promising characteristics with significant leakage current reduction at high voltage operation without sacrificing the forward current. Compared with the 3-D AlGaIn/GaN SBD in [11], the equivalent circuit [Fig. 1(b)] of the GET-SBD topology is composed of an SBD in series with a metal-insulator-semiconductor HEMT (MISHEMT). Fig. 1(c) shows the 2-D electric field distribution of the GET-SBD at -100 V. It is shown that the GET structure pinches off the GaN channel in the diode OFF-state and redistributes the electric field [9].

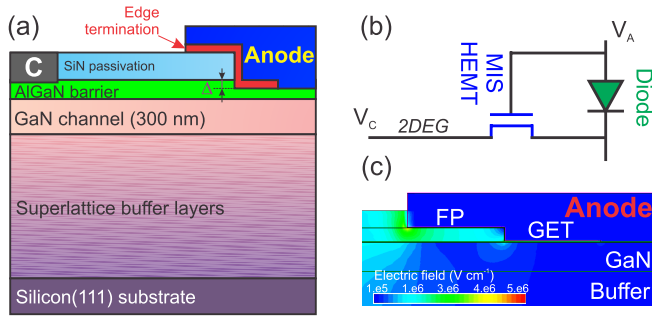


Fig. 1. (a) Schematic cross section of the AlGaIn/GaN GET-SBDs fabricated on a superlattice-based buffer. (b) Equivalent circuit of the GET-SBD composed of an MISHEMT structure embedded in the anode trench in series with the SBD. (c) 2-D electric field simulation of the anode region at a reverse voltage of -100 V.

To obtain a better electrostatic control in the GET region, a more positive threshold voltage (V_{TH}) in this embedded MISHEMT structure is highly desirable. The approach of sufficient AlGaIn barrier recess in the gate area of the AlGaIn/GaN MISHEMT to obtain the enhancement-mode transistors has been widely used in the literature [8], [12]. An atomic layer etching (ALE) process, composed of a sequential oxidation and removal of the AlGaIn barrier, has been developed to allow AlGaIn barrier recess with controlled accuracy. With the increase of the number of ALE cycles in the gate area, more positive V_{TH} of the MISHEMT can be obtained [8].

In this paper, we demonstrate further reverse leakage reduction of GET-SBDs by applying various ALE cycles (0, 2, and 6 ALE) for anode recessing to improve the pinching off capability at the GET region. TCAD electrical simulations confirm the impact of ALE on the reverse leakage current and the idea of better electrostatic control of the channel with increasing number of ALE cycles. Statistical variation of leakage current, turn-ON and forward voltages with ALE cycles is analyzed for GET-SBDs on 3 otherwise identical 200-mm GaN-on-Si wafers. Moreover, the dynamic characteristics of GET-SBD with three different ALE cycles are investigated.

II. EXPERIMENTAL DETAILS

A. Epi-Structure and Device Processing

The AlGaIn/GaN epitaxial layers were grown on 200-mm silicon wafers by metalorganic chemical vapor deposition (MOCVD). The epi-structure consists of a 10-nm $Al_{0.25}Ga_{0.75}N$ barrier, a 0.5-nm AlN spacer, a 300-nm GaN channel layer, a 1- μ m GaN:C back-barrier, a 1.65- μ m C-doped AlGaIn/AlN superlattice buffer [13], 40-nm $Al_{0.3}Ga_{0.7}N$ transition layer, and a 200-nm AlN nucleation layer on p-type Si(111) substrates. A 5-nm *in situ* Si_3N_4 , grown in the MOCVD chamber, is used as the passivation capping layer of the wafers. The surface of the entire epi-stack was then encapsulated by a 140-nm Si_3N_4 layer by means of rapid thermal chemical vapor deposition (RTCVD).

We used an anode-first approach for the device process. The removal of the RTCVD and *in situ* Si_3N_4 passivation layer in the anode region was done by SF_6 dry etching. To perform ALE in the anode region, we used a BCl_3 -based

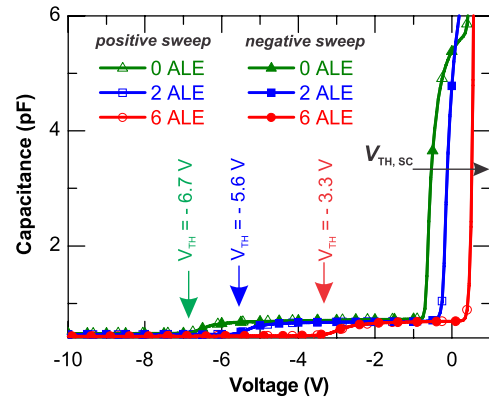


Fig. 2. Bidirectional capacitance–voltage measurements for GET-SBDs with three different ALE cycles. More ALE cycles lead to a more positive threshold voltage of the MISHEMT and the diode.

plasma at low bias power to precisely etch (~ 1 nm/cycle) the AlGaIn barrier. Prior to the Si_3N_4 deposition in the anode trench to form the edge termination, three ALE conditions (0, 2, and 6 cycles) were applied on three identical wafers, the remaining AlGaIn barrier thickness was 10, 8, and 4 nm, respectively. The edge termination was then fabricated by depositing a 25-nm plasma-enhanced atomic layer deposition (PEALD)- Si_3N_4 in the anode trench on top of the recessed or nonrecessed AlGaIn barrier. The center region was opened to allow the formation of an SC on top of the AlGaIn barrier. Thus an MISHEMT structure is formed next to the Schottky junction, as shown in Fig. 1(a) and (b). Before the deposition of the anode metal, an *in situ* N_2 plasma cleaning step was given to remove traps at the exposed AlGaIn surface [14], [15]. The anode metal stack consists of an ionized metal plasma physical vapor deposited (PVD) TiN-based metal [7]. A stack of Ti/Al-based metal was used for the cathode contacts, which was annealed at 550 °C [2].

Capacitance–voltage (C – V) measurements were performed at 100 kHz on the GET-SBD from the three wafers with different ALE conditions. Fig. 2 shows the bidirectional C – V measurements (from -10 to 0.5 V) for GET-SBDs with three different ALE cycles, no hysteresis is observed indicating that negligible electron trapping occurs in this voltage range. Furthermore, more ALE cycles applied at the anode area leads to a more positive V_{TH} for the MISHEMT ($V_{TH,MISHEMT}$) and the diode ($V_{TH,SC}$). The positive shifts in V_{TH} lead to a reduction of 2-DEG density in the GaN channel. In particular, after six ALE cycles, the 2-DEG is still present (partially depleted) in the GaN channel under the GET region at equilibrium (at 0 V), whereas it is completely depleted under the Schottky metal. The threshold voltages, contact resistance (R_C), and 2-DEG sheet resistance (R_{sheet}) for the three wafers are listed in Table I.

B. Measurement and TCAD Setup

The GET-SBDs studied in this paper have an SC length (L_{SC}), an anode finger width, and an anode-to-cathode distance (L_{ac}) of 6, 100, and 5 μ m, respectively. The lateral dimension of the gated edge termination in the anode trench is 1 μ m. The forward and reverse (up to -100 V)

TABLE I
COMPARISON OF EXTRACTED $V_{TH,MISHEMT}$, $V_{TH,SC}$, MEDIAN R_C , AND R_{sheet} FOR THE THREE WAFERS WITH THREE ALE SPLITS

	# cycles	Remaining AlGaIn thickness (nm)	$V_{TH,MISHEMT}(V)$	$V_{TH,SC}(V)$	$R_C (\Omega \times mm)$	$R_{sheet} (\Omega/\square)$
Wafer1	0 ALE	10	-6.7	-0.7	0.489	369.04
Wafer2	2 ALE	8	-5.6	-0.4	0.486	371.13
Wafer3	6 ALE	4	-3.3	0.35	0.539	370.86

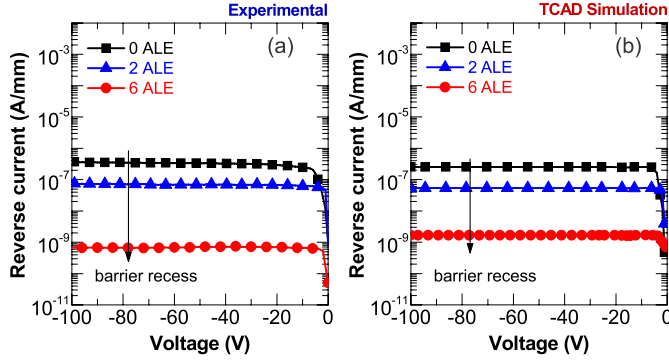


Fig. 3. (a) Typical OFF-state characteristics of GET-SBDs with three different ALE cycles. (b) TCAD electrical simulations confirm the trend of leakage reduction with ALE cycles for anode recessing, and a good overlay between experimental and simulation is shown as well.

characterizations of the GET-SBDs have been performed by using an Agilent 4073 Ultra Advanced Parametric Tester. The BD and pulsed I - V measurements were done with an Agilent B1505A Semiconductor Device Analyzer. The substrate and the anode were connected to ground, and the voltage was applied at the cathode contact to minimize the trapping phenomenon [16]. All the measurements were performed at 25 °C.

In order to verify the better electrostatic control with more ALE cycles, a calibrated TCAD device simulator (Synopsys Sentaurus Device [17]) has been used to enable electrical simulations on AlGaIn/GaN GET-SBD. In the simulator, two discrete donor traps at $E_C - 1.65$ eV and $E_C - 1$ eV, were defined at the AlGaIn barrier/ Si_3N_4 material interface with a density equal to $2.5 \times 10^{13} \text{ cm}^{-2}$ (similar to [18]) and $1 \times 10^{13} \text{ cm}^{-2}$, respectively. The anode work function was set to be 4.6 eV. A nonlocal tunneling model [19] has been used and defined at the anode contact, since tunneling process is the dominant mechanism in the reverse leakage current of AlGaIn/GaN diodes [9].

III. RESULTS AND DISCUSSION

A. Better Electrostatic Control With ALE

The experimental reverse leakage currents of GET-SBDs with different ALE cycles are shown in Fig. 3(a). A clear trend of reverse leakage reduction with the number of ALE cycles is demonstrated. With a remaining AlGaIn barrier of 4 nm, a leakage of ~ 1 nA/mm at -100 V is achieved in GET-SBDs with 25-nm Si_3N_4 edge termination. TCAD simulations, shown in Fig. 3(b), confirm the trend in leakage current with ALE and show a good overlay with the experimental results.

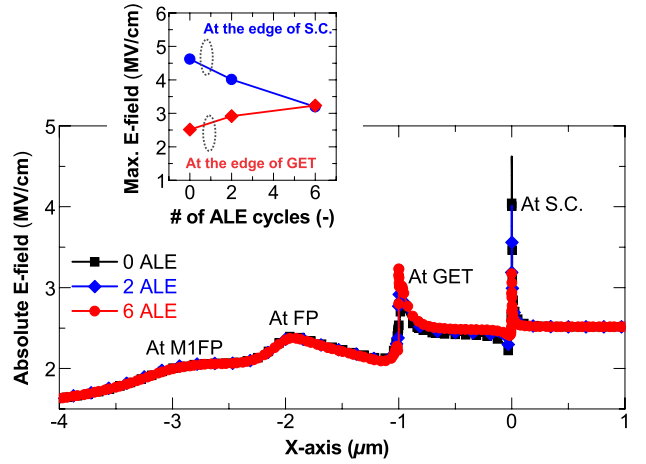


Fig. 4. Electric field distribution in the AlGaIn barrier (0.5 nm away from the anode contact) under a reverse voltage of -100 V for the GET-SBD with three different recess conditions. Inset: maximal electric field values at the edge of the SC and the edge of the GET for these three recess conditions.

In the OFF-state, the diode leakage current is dominated by the electron tunneling from the anode contact through the AlGaIn barrier, into the depleted GaN channel [9]. The electric field peak at the anode edge determines the band bending and electron injection in this tunneling process. The trend of leakage reduction with more ALE cycles can be explained by the lower number of injected electrons, although the AlGaIn barrier is thinner after recess. In order to verify this, the simulated electric field distribution (at reverse voltage $V_R -100$ V) in the AlGaIn barrier (0.5 nm away from the anode contact) for three recess conditions is shown in Fig. 4. With the embedded edge termination, the field plate (FP) overhang on the passivation layer and the metal-1 FP, the OFF-state electric field is redistributed. The peak value of the electric field at the anode edge, which directly determines the electron injection, is replotted in the inset graph in Fig. 4. It shows that the peak E -field at the anode edge reduces with the number of ALE cycles, which confirms the trend of leakage reduction. Furthermore, the inset graph of Fig. 4 shows that the electric field peak in the Si_3N_4 at the edge of the GET structure increases with the number of ALE cycles.

At fixed reverse voltage, the inset graph of Fig. 4 shows the interplay between the maximal electric field at the anode edge and the one at the edge of the GET structure. It confirms that anode recessing lowers the peak E -field at the anode edge with the cost of increasing the peak E -field in the Si_3N_4 dielectric. As the electric field at the edge of the GET increases with the number of ALE cycles, the channel is better pinched off in the recessed GET-SBDs. This gives another

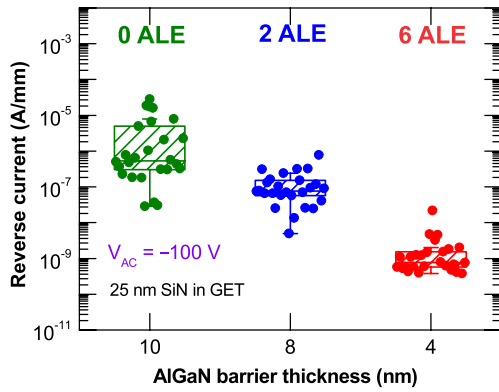


Fig. 5. Statistical evaluation of the leakage current (at V_R of -100 V) for GET-SBDs with three different ALE conditions over the 200-mm wafers.

perspective to understand the leakage mechanism. With a more positive $V_{TH,MISHEMT}$ in the GET region, a better electrostatic control of the channel can be achieved. Due to the 2-D operating principle, the electric field peak at the anode edge reduces when a better electrostatic control is reached in the GET region.

Fig. 5 shows the statistical plot of the leakage current (at anode-to-cathode voltage V_R of -100 V) for the GET-SBDs with the three ALE cycles. In these measurements, data of 26 GET-SBDs over the 200-mm GaN-on-Si wafers were collected. The statistical plot confirms that recessed GET-SBDs have better electrostatic control in the GET region to pinch-off the channel and reduce the electron injection from the anode contact. Compared with nonrecessed GET-SBDs, a leakage suppression by 2-3 orders of magnitude can be achieved in the GET-SBDs with six ALE cycles applied. Moreover, it is worth noting that a reduced reverse leakage spread is achieved when more ALE cycles are applied. When no ALE is applied, the initial large spread in the leakage of nonrecessed GET-SBDs may be due to the thickness variation of the PEALD- Si_3N_4 . When there is a $V_{TH,MISHEMT}$ variation in the GET region (i.e., due to thickness variation), the electrostatic control of the GET-SBD in the OFF-state operation can vary from die-to-die across the wafer. The spread reduction with more ALE cycles can be understood as the dominant pinching off capability in the recessed GET region becomes more uniform. Once the channel is fully pinched off due to a better electrostatic control, the leakage of GET-SBDs is suppressed and the cause for the initial spread of the leakage diminishes.

BD measurements were performed on the GET-SBDs with different ALE cycles, the results are shown in Fig. 6. The leakage shown in Fig. 6 is the current from the anode electrode. It is believed that the BD mechanism is related to the damage at the anode contact. The inset graph in Fig. 6 shows the statistics of BV for the three conditions. The BV shown in Fig. 6 corresponds to the voltage when the diode suffers from hard BD. All the GET-SBDs with different ALE cycles break approximately at V_R of -800 V. It points out that they all break down due to the same mechanism. Furthermore, we observe a rising leakage in these three cases when the V_R exceeds a certain value (i.e., kink voltage V_{kink}). As we understood that the channel is pinched off in the GET region,

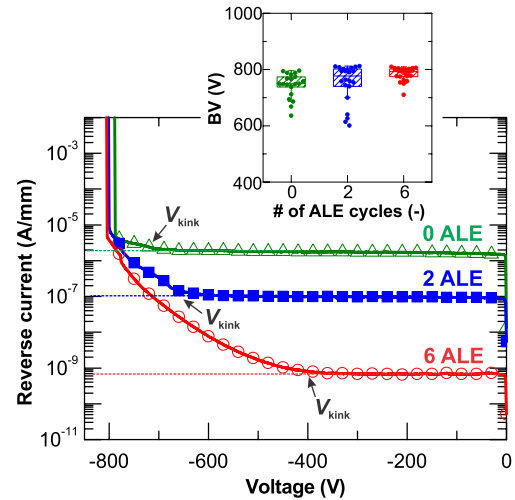


Fig. 6. BD measurement on the GET-SBDs with different ALE cycles. An increase of leakage current was observed in three cases. Inset: statistics of BV for GET-SBDs with three different ALE conditions.

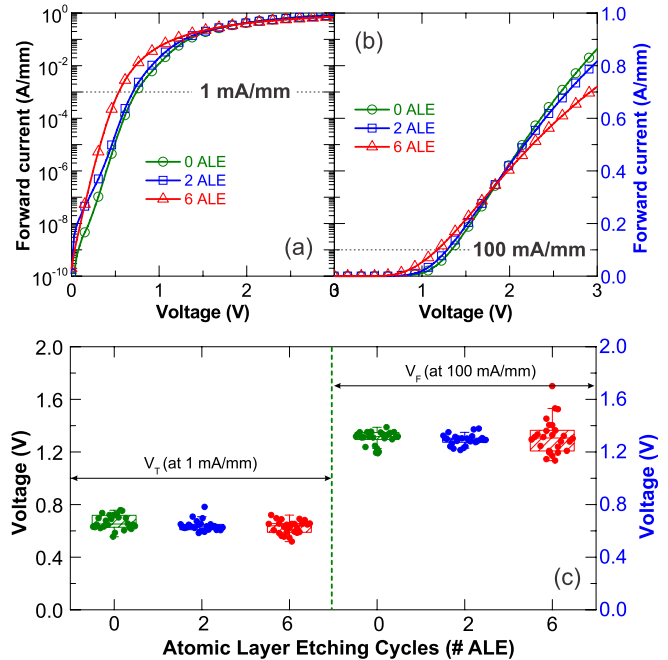


Fig. 7. Forward characteristics of three GET-SBDs with different ALE conditions plotted on (a) semilogarithmic scale and (b) linear scale. (c) Extracted turn-ON voltage (at forward current 1 mA/mm) and forward voltage (at forward current 100 mA/mm) for the three wafers.

the leakage current through the PEALD- Si_3N_4 can be dominant when the voltage across the dielectric is sufficiently high. This describes exactly what happened for the rising leakage in the GET-SBDs in Fig. 6. When the V_R is below the value of the V_{kink} , the leakage for the three GET-SBDs is almost independent of the voltage due to the electrostatic control of the GET structure. We drew three parallel lines in Fig. 6 exhibiting the intrinsic leakage level of the three GET-SBDs, which are in alignment with the statistical value in Fig. 5. In this regime, the intrinsic diode leakage (at the anode edge) dominates. As the V_R increases, the voltage across

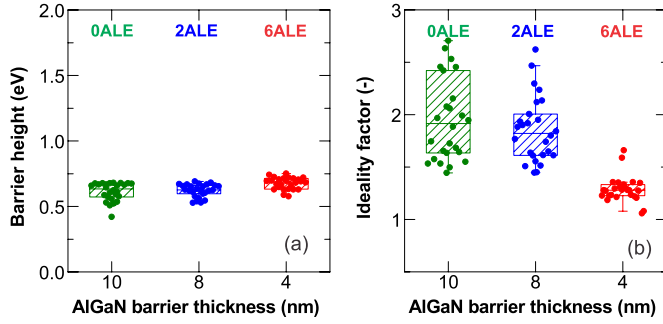


Fig. 8. Statistics of (a) extracted barrier height and (b) ideality factor for the GET-SBDs with three different ALE conditions.

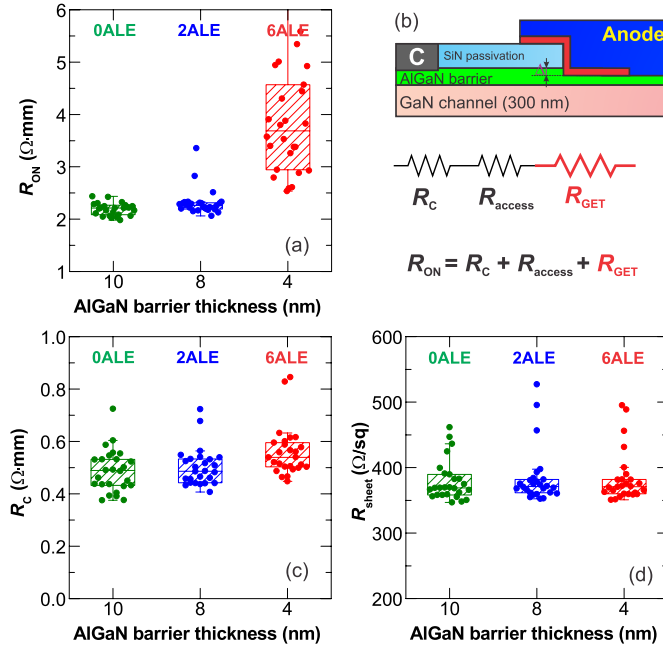


Fig. 9. (a) Statistics of R_{ON} for the three wafers. (b) Schematic of the recessed GET-SBD and the decomposition of R_{ON} . Statistics of (c) contact resistance R_C and (d) 2-DEG sheet resistance R_{sheet} .

the PEALD- Si_3N_4 rises. At a certain moment (i.e., at V_{kink}), the parasitic leakage through the Si_3N_4 becomes dominant over the diode leakage and eventually leads to the BD of the device. The revealed ALE-dependent V_{kink} is related to the different voltage drop or E -field in the Si_3N_4 and most likely their leakage levels for the three conditions.

B. Impact of ALE on Forward Characteristics

The typical forward characteristics of three GET-SBDs with different ALE cycles are presented in Fig. 7(a) and (b). With the ALE process in the anode region, the probability for electrons in the channel to tunnel through the remaining thin AlGaIn barrier becomes higher. As shown in Fig. 7(a), there is a negative shift of the forward I - V characteristics for GET-SBD with more ALE cycles. However, the anode recessing leads to the reduction of the 2-DEG density in the anode area (under the GET region and the SC). This results in the increase of the ON-resistance, which is reflected in the slope changes in the linear-scale graph in Fig. 7(b). The extracted

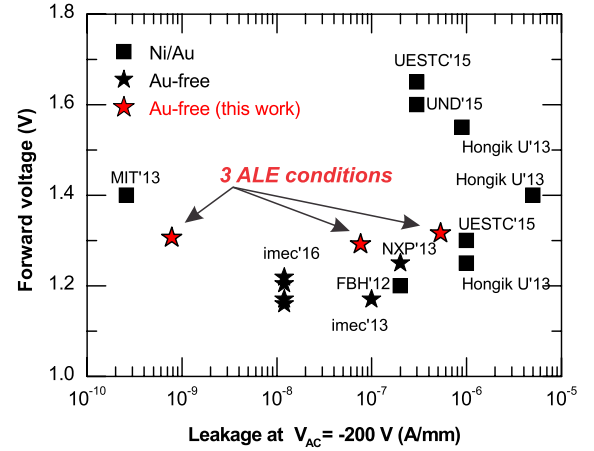


Fig. 10. Benchmarking graph of the leakage current at V_R of -200 V (the leakage for the work in [11] was taken at -127 V due to an early device BD) and the forward voltage of lateral AlGaIn/GaN Schottky diodes with Ni/Au-based and Au-free technology.

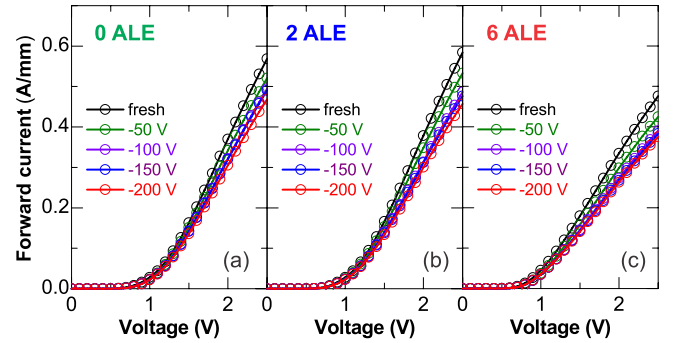


Fig. 11. Typical pulsed I - V characteristics of GET-SBDs with different recess conditions.

TABLE II
SUMMARY OF THE MEDIAN V_T , V_F , AND R_{ON} FOR THE THREE WAFERS WITH THREE ALE SPLITS

# cycles	V_T (V)	V_F (V)	R_{ON} ($\Omega \times \text{mm}$)
0 ALE	0.652	1.316	2.21
2 ALE	0.629	1.292	2.26
6 ALE	0.638	1.307	3.69

ON-resistance for the three cases (0, 2, and 6 ALE) are 2.21, 2.26, and 3.69 $\Omega \times \text{mm}$, respectively. Fig. 7(c) shows the statistics of the turn-ON voltage (at a forward current of 1 mA/mm) and forward voltage (at 100 mA/mm) for GET-SBDs with three recess conditions. The median values of V_T , V_F , and R_{ON} for the three wafers are summarized in Table II. Negligible difference in the median values of V_T and V_F is found, taking into account the statistical distribution.

Fig. 7(c) shows a spread increase in V_F when six ALE cycles are applied. The evaluation of the spread in the apparent barrier height and ideality factor extracted for the three GET-SBDs based on thermionic emission model [20] shown in Fig. 8. With the increase of ALE cycles, the apparent barrier height shows a slight increase which may be related to the reduction of the 2-DEG density in the recessed anode

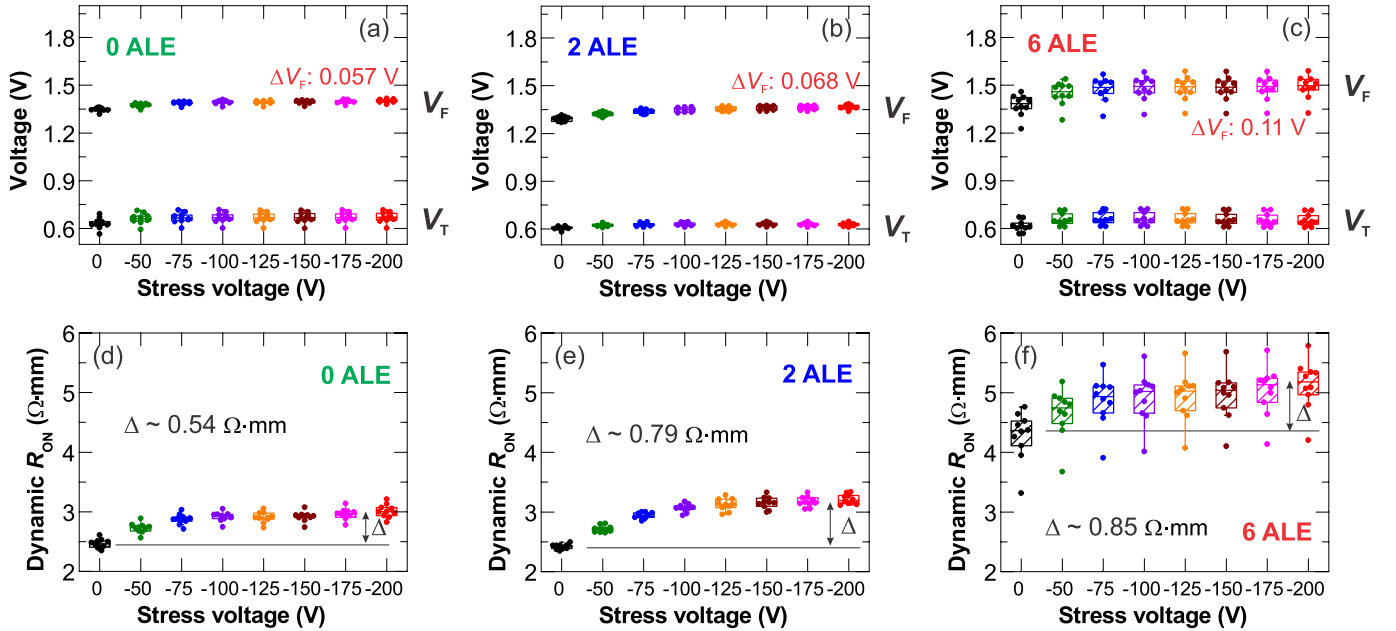


Fig. 12. (a)–(c) Statistical variation of V_T and V_F for GET-SBDs with the three different ALE conditions. (d)–(f) Dynamic R_{ON} of GET-SBDs with the three different ALE conditions.

region (positive shift of $V_{TH,SC}$). The spread in the apparent barrier height does not change with the number of ALE cycles. However, Fig. 8(b) shows that the extracted ideality factor and its spread reduce with the number of ALE cycles. It is most likely that the current transport mechanism depends strongly on the thickness of the remaining AlGaIn barrier. The large ideality factors for GET-SBDs with zero or two ALE cycles indicate that trap-assisted tunneling may be the dominant transport process in the forward operation. Based on the results in Fig. 8(a), we can conclude that the spread increase in V_F is not due to the variation of the apparent barrier height.

The forward voltage can be described as

$$V_F = V_T + R_{ON} \times I_{ON}. \quad (1)$$

The larger spread in V_F can be ascribed to be the variation in R_{ON} , since the V_T variation is shown to be less ALE-dependent. Fig. 9(a) shows the statistics of R_{ON} for the three wafers, which confirms the large spread of R_{ON} for GET-SBDs with six ALE cycles. As is shown in Fig. 9(b), the R_{ON} of the GET-SBD can be decomposed to be the sum of R_C , R_{sheet} , and R_{GET} , where R_{GET} is highly dependent on the ALE cycles. The statistics of R_C and R_{sheet} for the three wafers are shown in Fig. 9(c) and (d), respectively. These results exclude that the spread in R_{ON} is due to the wafer variations. As a consequence, the ALE-dependent R_{ON} and its spread in Fig. 10(a) can be attributed to R_{GET} . With more ALE applied, it results in more variation in the remaining AlGaIn barrier thickness. This leads to the variations of the 2-DEG density and the electron mobility in the channel.

Fig. 10 shows the benchmarking graph of the leakage current (at V_R of -200 V) and the forward voltage of lateral AlGaIn/GaN SBDs from the literature. In this paper, we show that a gradual leakage reduction can be further achieved in the

GET-SBD by applying more ALE cycles in the anode region and improving the electrostatic control for the diode OFF-state operation. Compared with the sophisticated 3-D anode design in [11] with Ni/Au as the anode metallization, we are able to fabricate sufficiently low-leakage AlGaIn/GaN SBDs in a Au-free technology without showing early device BD.

C. Dynamic Stability of GET-SBDs With ALE

To evaluate the dynamic stability of GET-SBDs with different ALE conditions, pulsed I – V measurements have been performed over the 200-mm wafers. More details regarding the measurement procedure can be found in [21]. Fig. 11 shows the typical pulsed forward I – V characteristics for different prebias conditions of the three GET-SBDs. All the GET-SBDs with different ALE conditions show relatively stable forward characteristics without total current collapse or pronounced dynamic R_{ON} degradation. The ALE-dependent dynamic V_T , V_F , and R_{ON} are shown in Fig. 12. As indicated in Fig. 12(a)–(c), an ALE-dependent dynamic V_F increase is observed. With the increase of the stress voltages, the turn-ON voltage shows very stable characteristics in Fig. 12(a)–(c). The forward voltage increase is mainly due to the dynamic R_{ON} increase as is shown in Fig. 12(d)–(f). The ALE-dependent R_{ON} spread is also confirmed in Fig. 12(d)–(f). With more ALE cycles applied, it is possible that more electrons are trapped in the vicinity of the anode contact (i.e., at the edge of GET) under OFF-state stress conditions.

IV. CONCLUSION

This paper demonstrates a gradual reverse leakage current reduction of the GET-SBD architecture by improving the electrostatic control at the GET region through increasing number of anode recessing cycles. The trend of leakage reduction with the number of ALE cycles has been confirmed by the statistical

analysis of the experimental data and verified by the TCAD electrical simulations. GET-SBDs with more ALE cycles (i.e., six ALE) achieved a median leakage value of ~ 1 nA/mm and a forward voltage of 1.3 V. Due to the better electrostatic control, the reverse leakage current of GET-SBD maintains a stable value until the moment when the leakage through the PEALD-Si₃N₄ dielectric becomes dominant and eventually leads to BD. Further analysis of the ON-state characteristics shows that the ALE process can create variations at the AlGaIn surface, leading to a larger spread of the V_F and R_{ON} when six ALE cycles were applied in the GET-SBD. The R_{ON} variation can be the summed effect of 2-DEG density and mobility variations in the GaN channel under the GET region. The dynamic characterization of GET-SBDs shows stable forward characteristics and parameters and a small ALE-dependence.

ACKNOWLEDGMENT

The authors would like to thank Prof. T. Palacios at the Massachusetts Institute of Technology for the fruitful discussions and suggestions.

REFERENCES

- [1] E. Bahat-Treidel *et al.*, "Fast-switching GaN-based lateral power Schottky barrier diodes with low onset voltage and strong reverse blocking," *IEEE Electron Device Lett.*, vol. 33, no. 3, pp. 357–359, Mar. 2012.
- [2] S. Lenci *et al.*, "Au-free AlGaIn/GaN power diode on 8-in Si substrate with gated edge termination," *IEEE Electron Device Lett.*, vol. 34, no. 8, pp. 1035–1037, Aug. 2013.
- [3] M. Zhu *et al.*, "1.9-kV AlGaIn/GaN lateral Schottky barrier diodes on silicon," *IEEE Electron Device Lett.*, vol. 36, no. 4, pp. 375–377, Apr. 2015.
- [4] J. Hu *et al.*, "Current transient spectroscopy for trapping analysis on Au-free AlGaIn/GaN Schottky barrier diode," *Appl. Phys. Lett.*, vol. 106, no. 8, pp. 083502-1–083502-4, Feb. 2015.
- [5] S. L. Selvaraj, A. Watanabe, A. Wakejima, and T. Egawa, "1.4-kV breakdown voltage for AlGaIn/GaN high-electron-mobility transistors on silicon substrate," *IEEE Electron Device Lett.*, vol. 33, no. 10, pp. 1375–1377, Oct. 2012.
- [6] M. Van Hove *et al.*, "CMOS process-compatible high-power low-leakage AlGaIn/GaN MISHEMT on silicon," *IEEE Electron Device Lett.*, vol. 33, no. 5, pp. 667–669, May 2012.
- [7] J. Hu *et al.*, "Performance optimization of Au-free lateral AlGaIn/GaN Schottky barrier diode with gated edge termination on 200-mm silicon substrate," *IEEE Trans. Electron Devices*, vol. 63, no. 3, pp. 997–1004, Mar. 2016.
- [8] B. De Jaeger *et al.*, "Au-free CMOS-compatible AlGaIn/GaN HEMT processing on 200 mm Si substrates," in *Proc. 24th Int. Symp. Power Semiconductor Devices ICs (ISPSD)*, Jun. 2012, pp. 49–52.
- [9] J. Hu, S. Lenci, S. Stoffels, B. De Jaeger, G. Groeseneken, and S. Decoutere, "Leakage-current reduction and improved on-state performance of Au-free AlGaIn/GaN-on-Si Schottky diode by embedding the edge terminations in the anode region," *Phys. Status Solidi C*, vol. 11, nos. 3–4, pp. 862–865, 2014.
- [10] Y. Zhang *et al.*, "Origin and control of OFF-state leakage current in GaN-on-Si vertical diodes," *IEEE Trans. Electron Devices*, vol. 62, no. 7, pp. 2155–2161, Jul. 2015.
- [11] E. Matioli, B. Lu, and T. Palacios, "Ultralow leakage current AlGaIn/GaN Schottky diodes with 3-D anode structure," *IEEE Trans. Electron Devices*, vol. 60, no. 10, pp. 3365–3370, Oct. 2013.
- [12] M. Kanamura *et al.*, "Enhancement-mode GaN MIS-HEMTs with n-GaN/i-AlN/n-GaN triple cap layer and high- k gate dielectrics," *IEEE Electron Device Lett.*, vol. 31, no. 3, pp. 189–191, Mar. 2010.
- [13] S. Stoffels *et al.*, "The physical mechanism of dispersion caused by AlGaIn/GaN buffers on Si and optimization for low dispersion," in *Proc. IEEE Int. Electron Devices Meeting (IEDM)*, Dec. 2015, pp. 35.4.1–35.4.4.
- [14] S. Lenci, J. Hu, M. Van Hove, N. Ronchi, and S. Decoutere, "Improvement of the dynamic characteristics of Au-free AlGaIn/GaN Schottky diodes on 200 mm Si wafers by surface treatments," in *Proc. IEEE 26th Int. Symp. Power Semiconductor Devices IC's (ISPSD)*, Jun. 2014, pp. 265–268.
- [15] J. Hu *et al.*, "Physical origin of current collapse in Au-free AlGaIn/GaN Schottky barrier diodes," *Microelectron. Rel.*, vol. 54, nos. 9–10, pp. 2196–2199, Sep./Oct. 2014.
- [16] J. A. Croon, G. A. M. Hurkx, J. J. T. M. Donkers, and J. Šonkský, "Impact of the backside potential on the current collapse of GaN SBDs and HEMTs," in *Proc. IEEE 27th Int. Symp. Power Semiconductor Devices IC's (ISPSD)*, May 2015, pp. 365–368.
- [17] Synopsys, Device, Sentaurus. Inc., Dec. 2010.
- [18] B. Bakeroot *et al.*, "On the origin of the two-dimensional electron gas at AlGaIn/GaN heterojunctions and its influence on recessed-gate metal-insulator-semiconductor high electron mobility transistors," *J. Appl. Phys.*, vol. 116, no. 13, p. 134506, 2014.
- [19] Synopsys, User manual, ver. A-2009.06, Device, Sentaurus, Synopsys, 2009.
- [20] S. M. Sze and K. K. Ng, *Physics of Semiconductor Devices*. New York, NY, USA: Wiley, 2006.
- [21] J. Hu, S. Stoffels, S. Lenci, G. Groeseneken, and S. Decoutere, "On the identification of buffer trapping for bias-dependent dynamic RON of AlGaIn/GaN Schottky barrier diode with AlGaIn: C back barrier," *IEEE Electron Device Lett.*, vol. 37, no. 3, pp. 310–313, Mar. 2016.



Jie Hu (S'14) received the M.Sc. (*magna cum laude*) degree in nanoscience and nanotechnology from the Katholieke Universiteit Leuven, Leuven, Belgium, in 2012, where he is currently pursuing the Ph.D. degree in electrical engineering.

He has been with the Group of Power and Mixed Signal Technologies, Interuniversity Microelectronics Center, Leuven since 2012. In 2015, he was a Visiting Researcher with the Massachusetts Institute of Technology, Cambridge, MA, USA.



Steve Stoffels received the M.Sc. (*magna cum laude*) degree in applied physics from the Eindhoven University of Technology, Eindhoven, The Netherlands, in 2001, and the Ph.D. degree from the Katholieke Universiteit Leuven, Leuven, Belgium, in 2010.

He is currently a Device Engineer with the Interuniversity Microelectronics Center, Leuven, where he is involved in the R&D of high power GaN technology.



Silvia Lenci received the M.Sc. degree in electrical engineering from the University of Pisa, Pisa, Italy, in 2006, and the Ph.D. degree from the Department of Information Engineering, University of Pisa in 2010.

She is currently with the Interuniversity Microelectronics Center, Leuven, Belgium. Her current research interests include GaN-based high power electronic devices and sensors.



Brice De Jaeger received the B.S. and M.S. degrees in electrical engineering from the University of Ghent, Ghent, Belgium, in 1994 and 1997, respectively.

He has been a Research Engineer in different research departments with the Interuniversity Microelectronics Center, Leuven, Belgium, since 1997. His current research interests include GaN technology for power applications.



Nicolò Ronchi was born in Thiene, Italy. He received the Laurea degree in electronics engineering and the Ph.D. degree from the University of Padua, Padua, Italy, in 2008 and 2012, respectively.

He has been with the Interuniversity Microelectronics Center, Leuven, Belgium, as a Researcher in the Power and Mixed Signal Technologies Group since 2012.



Benoit Bakeroot received the M.Sc. degree in physics and the Ph.D. degree in electrical engineering from Ghent University, Ghent, Belgium, in 1997 and 2004, respectively.

He joined the Interuniversity Microelectronics Center, Leuven, Belgium, in 1998. Since 2010 he has been with GaN-on-Si devices. Since 2012, he has been a part-time Assistant Professor with Ghent University.



Andrea Natale Tallarico received the M.Sc. (magna cum laude) degree in electronic engineering from the University of Calabria, Rende, Italy, in 2012. He is currently pursuing the Ph.D. degree in electronic engineering with the University of Bologna, Bologna, Italy.

He was a Visiting Researcher with the Interuniversity Microelectronics Center, Leuven, Belgium, from 2012 to 2015. His current research interests include characterization and modeling of the semiconductor power devices reliability.

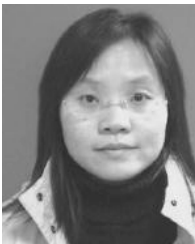


Guido Groeseneken (S'81–M'89–SM'95–F'05) received the M.Sc. degree in electrical engineering and the Ph.D. degree in applied sciences from the Katholieke Universiteit Leuven, Leuven, Belgium, in 1980 and 1986, respectively.

He joined the R&D Laboratory with the Interuniversity Microelectronics Center, Leuven, in 1987. Since 2001, he has been a Professor with the Department of Electrical Engineering, Katholieke Universiteit Leuven.



Dirk Wellekens received the M.Sc. degree in electrical engineering from the University of Ghent, Ghent, Belgium, in 1988 and the Ph.D. degree in applied sciences from the Katholieke Universiteit Leuven, Leuven, Belgium, in 1995. His Ph.D. thesis was titled Radiation and Reliability Aspects of Nonvolatile Memories. Since 2011, he has been working on GaN-based HEMTs for high power application.



Shuzhen You received the M.Sc. degree in electrical engineering from East China Normal University, Shanghai, China, in 2003, and the Ph.D. degree in electrical engineering from the Katholieke Universiteit Leuven, Leuven, Belgium, in 2012.

She joined the Interuniversity Microelectronics Center, Leuven in 2012, and currently a Device Engineer.



Stefaan Decoutere received the M.Sc. degree in electronic engineering and the Ph.D. degree from the Katholieke Universiteit Leuven, Leuven, Belgium, in 1986 and 1992, respectively.

In 1998, he was the Head of the Mixed Signal/RF Technology Group with the Interuniversity Microelectronics Center, Leuven. He has been with the GaN Power Device Technology Development since 2010, and in 2015 he became the Director of the GaN Technology Program.